Sliding-mode based Thrust Vector Control for Aircrafts

I. Martinez-Perez*, R. Garcia-Rodriguez, M.Vega-Navarrete, and L. Ramos-Velasco
Aeronautical Engineering Program and Postgraduate Program in Aerospacial Engineering
Universidad Politécnica Metropolitana de Hidalgo, Mexico

ABSTRACT

In recent years, aircraft research has focused its attention on propulsion systems that control vehicle attitude and flight path by Thrust Vector Control, TVC. The propulsion system with an integrated TVC mechanism is characterized to be provided better maneuverability to the aircraft through moments that allow rotating the flying vehicle helping to the attitude control. This paper proposes a sliding-mode-based TVC for an aircraft, focusing our attention on controlling the angle of attack through the convergence flight-path angle and the pitch angle. Using a rocket as a study system, we firstly present its dynamic model, assuming that the shape of the Earth is an ellipsoid. Then, a sliding-mode-based TVC is proposed to guarantee the aircraft attitude control, regulating the effective angle of attack. Finally, some result simulations show the performance of the proposed controller under different conditions.

1 INTRODUCTION

The initiative to make space flights more accessible and cheap has currently experienced rapid development on many topics as aerodynamics, fluids dynamics, propulsion, control, structural dynamics, to name but a few. In recent years, the propulsion systems that include TVC has attracted researchers' attention due to allowing change the flight path, correct a deviation from the desired trajectory, or change the altitude during the powered flight, [1], [2], [3]. In this way, TVC is used to pitch and yaw aircraft controls based on the main rocket nozzle. As part of the thrust system, the gimbal mechanism is in charge to move the nozzle in two or three degrees of freedom through actuators. Thus, for small aircraft, TVC based on electromechanical actuators is the most popular. Structural analysis, gimbal mechanism, control, and sizing are active areas of research of TVC.

In this paper, a thrust vector controller actuating in a single-engine rocket is proposed. Although operations of the rocket flight have many stages, we focus our attention on rocket landing, in particular, the flight control to compensate disturbance forces due to the influence of the environment and the parametric uncertainties of the rocket. Thus, the attitude rocket control with TVC is proposed using embedded motion equations of pitch attitude and inertial Z-axis drift position. Furthermore, from aircraft aerodynamics, it's known that the aircraft does not have a straight path to its destination; on the contrary, regularly, there is a slight deviation concerning the angle route or trajectory called the track, while its deviation is known as the angle of drift. Thus, the effects related to the wind must be added with the lifting and dragging to keep our vehicle stable. In this way, assuming some aircraft parameters are unknown and the wind speed is uncertain, a sliding-mode-based TVC is proposed to guarantee the pitch angle and drift position convergence. In addition, some stability conditions are guarantee using the Lyapunov theory. Finally, to validate the proposed approach, some simulations under different conditions are presented. The Sliding Mode Control (SMC) is characterized to provide robustness to parametric uncertainty and external perturbations using high-speed switching feedback control, [4], [5]. Due to its ability to deal with disturbance attenuation and robustness, the SMC is used commonly in flight control design or in combination with other approaches as backstepping or adaptive control. [6], [7], [8], [9], [10], [11].

This paper is organized as follows. In Section 2, the mathematical rocket model is presented with an integrated TVC system. In Section 3, a sliding mode control to guarantee the convergence of angle of attack through the convergence flight-path angle and the pitch angle is proposed. In Section 4, simulation results are presented under different conditions. Finally, some conclusions are presented in Section 5.

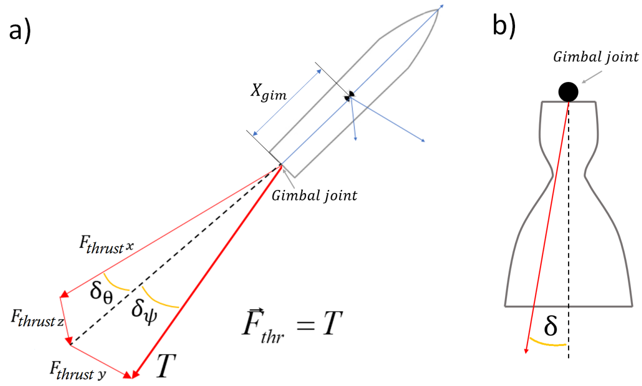

Figure 1: a) Aircraft with an integrated TVC mechanism, b) Gimbal mechanism: A gimbal is essentially a universal joint.

*Email address: 192220109@upmh.edu.mx

2 ROCKET DYNAMICAL MODEL

In this section, we present the rigid body analysis to obtain the rocket non-linear motion equations.

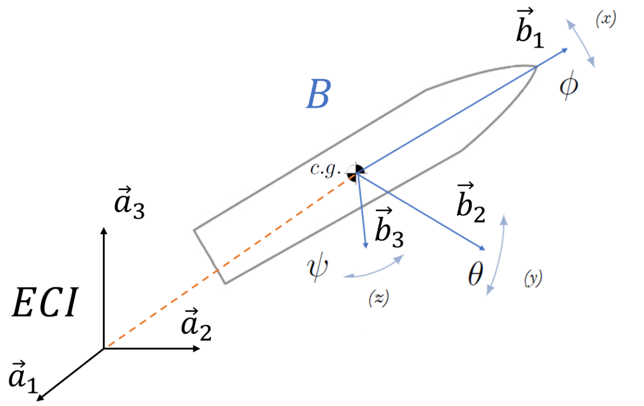

Figure 2: Reference system B (rocket) relative to ECI system.

2.1 *Rotational kinematics*

From the rotational kinematics, we describe the orientation of the aircraft by the Euler angles: roll (ψ), pitch (θ), and yaw (ϕ), see Figure 2, [12]. We start defining two reference systems: the Earth-Centered Inertial system (ECI) and the Body system (B) that refers to the aircraft frame. So, the rotational kinematics of the rocket to ECI frame is defined as:

$$\begin{bmatrix} \dot{\phi} \\ \dot{\theta} \\ \dot{\psi} \end{bmatrix} = \frac{1}{\cos\theta} \begin{bmatrix} \cos\theta & \sin\phi\sin\theta & \cos\phi\sin\theta \\ 0 & \cos\phi\cos\theta & -\sin\phi\cos\theta \\ 0 & \sin\phi & cos\phi \end{bmatrix} \begin{bmatrix} p \\ q \\ r \end{bmatrix} \tag{1}$$

where p, q, r represents the components of angular velocity.

2.2 *Translational Dynamics*

In this part, we will define the forces that act on the rocket. Specifically, we refer to the thrust force ($\vec{F}_{thrust}$), aerodynamic force ($\vec{F}_{aer}$) defined concerning the reference system B (Body) while the gravity force ($\vec{F}_g$) respect to ECI reference system. Applying the Second law's Newton (for a constant mass) concerning the ECI reference system, we have that

$$\begin{aligned} \vec{a} &= \begin{bmatrix} \ddot{x} \\ \ddot{y} \\ \ddot{z} \end{bmatrix} = \frac{1}{m}\vec{F} \\ &= \frac{1}{m}\left[T^B_{ECI}(\vec{F}_{aer} + \vec{F}_{thrust}) + \vec{F}_g\right] \end{aligned} \tag{2}$$

where T^B_{ECI} is the transformation matrix defined by $T^B_{ECI} = R(x,\phi)R(y,\theta)R(z,\psi)$ and $R(x,\phi), R(y,\theta), R(z,\psi)$ are the rotation matrices corresponding to each axis.

In the following sub-section, we will show how are defined the principal force applied to the rocket, that is, $\vec{F}_{thrust}$, $\vec{F}_{aer}$, and $\vec{F}_g$.

2.2.1 Thrust Force

The thrust delivered by the rocket engine can be calculated by:

$$T = \dot{m}v_e + (P_e - P_0)A_e \tag{3}$$

where $\dot{m}v_e$ is the propellant burned escaping a constant velocity, $(P_e - P_0)A_e$ is the pressure difference, between inside the nozzle (P_e) and outside the nozzle (P_0), on an escape surface (A_e). Assuming that the thrust is constant T, we proceed to determine the thrust vector components, which allows us to define the TVC, see Figure 1a. Using the relationship of right triangles, from Figure 3 we can define the components of the TVC. Thus, the thrust y-component is defined as

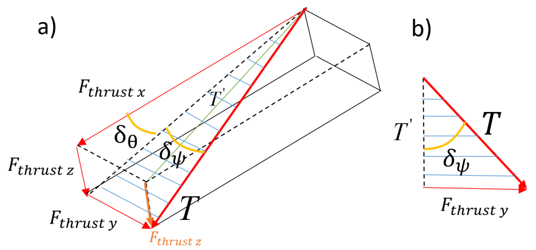

Figure 3: a) $\vec{F}_{thrust}$ Components b) y-component example

$$F_{thrust_y} = T\sin\delta_\psi \tag{4}$$

while the thrust z-component is given as

$$F_{thrust_z} = T\sin\delta_\theta \tag{5}$$

Finally, using that $T' = T\cos\delta_\psi$ we have that thrust x-component is given as

$$\begin{aligned} F_{thrust_x} &= T\prime\cos\delta_\theta \\ F_{thrust_x} &= T\cos\delta_\psi\cos\delta_\theta \end{aligned} \tag{6}$$

In this way, the $\vec{F}_{thrust}$, which include the TVC, is defined as:

$$\vec{F}_{thrust} = \begin{bmatrix} F_{thrust_x} \\ F_{thrust_y} \\ F_{thrust_z} \end{bmatrix} = \begin{bmatrix} T\cos\delta_\psi\cos\delta_\theta \\ T\sin\delta_\psi \\ T\sin\delta_\theta \end{bmatrix} \tag{7}$$

2.2.2 Aerodynamic Forces

When the rocket is in flight, two important aerodynamic forces are generated: the lift $\vec{L}$ produced by the rocket surfaces, and the drag $\vec{D}$ produced by the air resistance of these same surfaces. Assuming a simple geometry of the rocket, we have that the lift and drag forces can be defined as a normal force N, the axial force A, and a lateral slip force S, see Figure 4.

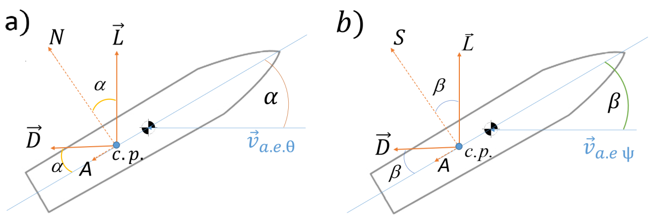

Figure 4: Aerodynamic force: a) xz plane, b) yz plane

Let the axial force A defined directly as $A = \frac{1}{2} C_A \rho V_{air}^2 \cdot surface$ where C_A represents the aerodynamic coefficient given A, ρ the density of the air, V_{air} the airspeed, and $surface$ the total surface where the air affects. For the normal and slip forces, we define them in terms of the real displacement and the wind disturbance (α_w), such that normal force N and the lateral slip force S are defined as:

$$N = N_\alpha \sin\alpha \tag{8}$$

$$S = S_\beta \sin\beta \tag{9}$$

where N_α is the the normal force dependent on the angle of attack α, S_β is the lateral slip force dependent on angle of slip β with $\alpha = \theta + \gamma_\theta + \alpha_{w_\theta}$ and $\beta = \psi + \gamma_\psi + \alpha_{w_\psi}$

In Figure 5 can be seen the actual speed and direction of displacement V, which is defined aerodynamically as the track of the rocket and the angle formed by it and the x axis, or y axis, generally known as the drift angle, $\gamma = \frac{\dot{z}}{V}$. From here, other terms arise, such as the effective wind velocity $\vec{v}_{a.e.}$, the wind disturbance $V_{p.a.}$, for pitch (θ) and roll (ψ) angles, respectively. Thus, the normal force and the lateral slip force affected by the angle of attack are defined as:

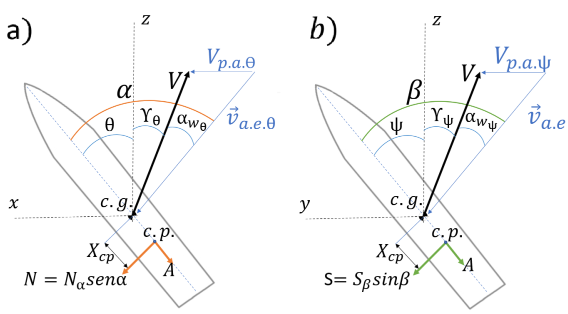

Figure 5: Aerodynamic force with wind disturbance: a) xz plane, b) yz plane

$$N_\alpha = \frac{1}{2} C_N \rho V_{air}^2 \cdot surface \tag{10}$$

$$S_\beta = \frac{1}{2} C_S \rho V_{air}^2 \cdot surface \tag{11}$$

where C_N is the aerodynamic coefficient given the normal force, N, and C_S represents the aerodynamic coefficient given lateral slip force, S. In this way, the aerodynamic forces can be defined as:

$$\vec{F}_{aer} = \begin{bmatrix} F_{aer_x} \\ F_{aer_y} \\ F_{aer_z} \end{bmatrix} = \begin{bmatrix} -A \\ S \\ -N \end{bmatrix} = \begin{bmatrix} -A \\ S_\beta \sin\beta \\ -N_\alpha \sin\alpha \end{bmatrix} \tag{12}$$

REMARK. The components (N,A,S) can be used for ideal aerodynamic performance.

2.2.3 Gravity Force

Unlike other approaches, in this case, we consider the earth's geometry as a WGS84 ellipsoid, proposed in 1984 by the World Geodesic System, currently called Geoid. This assumption is based on the principal rocket mission schedule. In Figure 6 we can observe a cross-section of the ellipsoid earth geometry, where the gravitational acceleration is modeled in geocentric inertial coordinates, [13], getting the gravity as $\mathbf{g} = g_r + g_\lambda$, where each component is defined as:

$$\begin{aligned} g_r &= -\frac{\mu}{r^2}[1 - 3J_2(\frac{R_0}{r})^2 P_2(\cos\Phi_c) \qquad (13)\\ &- 4J_3(\frac{R_0}{2})^3 P_3(\cos\Phi_c) - 5J_4(\frac{R_0}{r})^4 P_4(\cos\Phi_c)] \\ g_\lambda &= -3\frac{\mu}{r^2}(\frac{R_0}{r})^2 \sin\Phi_c \cos\Phi_c [J_2 + \frac{1}{2} J_3(\frac{R_0}{r}) \sec\Phi_c \\ & (5\cos^2\Phi_c - 1) + \frac{5}{6} J_4(\frac{R_0}{r})^2 (7\cos^2\Phi_c - 1)] \qquad (14) \end{aligned}$$

where $J_2 = 1.0826e^{-3}$, $J_3 - 2.54e^{-6}$ and $J_4 = -1.61e^{-6}$ are the oblateness terms (dimensionless) or spherical harmonics of an ellipsoid earth, approximated by empirical data to better approximate the earth geometry.

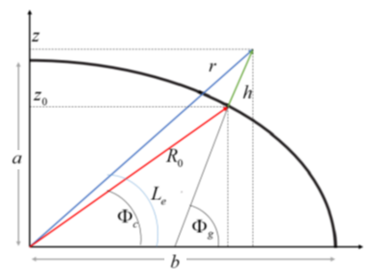

Figure 6: Gravity (Ellipsoidal Earth)

Taking the corresponding transformation of gravity in the geocentric coordinate system to the Cartesian coordinate system about the ECI reference system, [14], we have:

$$g_x = -\frac{\mu}{r^2}\left[1 + \frac{3}{2} j_2 (\frac{R_0}{r})^2 (1 - 5(\frac{z}{r})^2)\right] \frac{x}{r} \tag{15}$$

$$g_y = -\frac{\mu}{r^2}\left[1 + \frac{3}{2} j_2 (\frac{R_0}{r})^2 (1 - 5(\frac{z}{r})^2)\right] \frac{y}{r} \tag{16}$$

$$g_z = -\frac{\mu}{r^2}\left[1 + \frac{3}{2} j_2 (\frac{R_0}{r})^2 (3 - 5(\frac{z}{r})^2)\right] \frac{z}{r} \tag{17}$$

where μ is the universal gravitational parameter, R_0 the distance between the surface location on Earth and the center of Earth, h the height from Earth's surface to the rocket, r the distance between the rocket and the earth center.

Finally, we know that $\vec{F}_g = m\vec{g}$, so the gravity force is defined as:

$$\vec{F}_g = m\begin{bmatrix} g_x \\ g_y \\ g_z \end{bmatrix} = m\begin{bmatrix} -\frac{\mu}{r^2}\left[1+\frac{3}{2}j_2(\frac{R_0}{r})^2(1-5(\frac{z}{r})^2)\right]\frac{x}{r} \\ -\frac{\mu}{r^2}\left[1+\frac{3}{2}j_2(\frac{R_0}{r})^2(1-5(\frac{z}{r})^2)\right]\frac{y}{r} \\ -\frac{\mu}{r^2}\left[1+\frac{3}{2}j_2(\frac{R_0}{r})^2(3-5(\frac{z}{r})^2)\right]\frac{z}{r} \end{bmatrix} \quad (18)$$

2.3 *Rotational Dynamics*

From Euler's second law for a rotating rigid solid, which states that the rate of change of angular momentum $\dot{\vec{L}}$ about a fixed point (or center of mass of the body), is equal to the sum of the moments $\vec{M}$ that act on that body, we have that $\vec{M} = \dot{\vec{L}}$ where the angular momentum $\vec{L}$ is defined as $\vec{L} = \hat{J}\cdot\vec{\omega}$ with $\vec{\omega}$ the angular velocity and $\vec{J}$ the moment of inertia. Thus, the angular acceleration $\vec{\omega}$ is given as, [15]

$$\dot{\vec{\omega}} = \begin{bmatrix} \dot{p} \\ \dot{q} \\ \dot{r} \end{bmatrix} = \hat{J}^{-1}\left[\vec{M} - \vec{\omega}\times\left(\hat{J}\cdot\vec{\omega}\right)\right] \quad (19)$$

Due to the sum of the moments $\vec{M}$ acting on the rocket are produced by the thrust forces and the aerodynamic forces while the gravity acts uniformly over the entire rocket, it does not create a moment, we have that

$$\vec{M} = \vec{M}_{aer} + \vec{M}_{thrust} \quad (20)$$

where $\vec{M}_{aer} = \vec{r}_{c.p.} \times \vec{F}_{aer}$ represents the aerodynamic forces acting on center of pressure ($c.p.$) as the Figure 5, while $\vec{M}_{thrust} = \vec{r}_{gim} \times \vec{F}_{thrust}$ is the thrust force from the gimbal of the nozzle as the Figure 1 a) with $\vec{r}_{c.p.} = \begin{bmatrix} -X_{c.p.} & 0 & 0 \end{bmatrix}$ the distance between the $c.p.$ and the $c.g.$, and $\vec{r}_{gim} = \begin{bmatrix} -X_{gim} & 0 & 0 \end{bmatrix}$ the distance between the gimbal joint of the nozzle and the $c.g$. The gyro-axis is the center of gravity ($c.g.$).

It is correct to mention that the moment of inertia, produced by the rocket's opposition to moving, calculated by rocket geometry, is variable at each instant of time. So for simpler terms, it will be constant in the rotational dynamics. Now, if we align the axes of the body with the axes of the ECI reference frame, we can reduce the tensor as follows

$$\hat{J} = \begin{bmatrix} J_{xx} & 0 & 0 \\ 0 & J_{yy} & 0 \\ 0 & 0 & J_{zz} \end{bmatrix} \quad (21)$$

Substituting (21) and (20) in (19), we have that the rotational dynamics is defined as:

$$\begin{bmatrix} \dot{p} \\ \dot{q} \\ \dot{r} \end{bmatrix} = \begin{bmatrix} \frac{-qr(J_{zz}-J_{yy})}{J_{xx}} \\ \frac{[-X_{c.p.}N_\alpha \sin\alpha + X_{gim}T\sin\delta\theta - pr(J_{xx}-J_{zz})]}{J_{yy}} \\ \frac{[-X_{c.p.}S_\beta \sin\beta - X_{gim}T\sin\delta\psi - pq(J_{yy}-J_{xx})]}{J_{zz}} \end{bmatrix} \quad (22)$$

Finally, we have the complete rocket dynamical model composed of rotational kinematics, translational dynamics, and rotational dynamics. That is, the equations (1), (2) and (22), respectively.

2.4 *Rocket Model Reduction*

In this work, we focus on compensating the wind disturbance by controlling the attack angle by the convergence flight-path angle and pitch angle. Such that the longitudinal rocket dynamics will be used.

Given that depth in y-axis does not exist, since it is a plane, we have that angles ϕ and ψ, and their derivatives, are not considered. So we have that the slip S in this direction is zero. In this way, the control angle of the nozzle δ_ψ which moving in combination with planes xy and yz is zero. Thus, the rocket dynamics on the xz plane is given as:

$$\ddot{x} = [\cos\theta(T\cos\delta\theta - A) - \sin\theta(T\sin\delta\theta - N_\alpha\sin\alpha)]\frac{1}{m} + g_x$$
$$\ddot{z} = [(\sin\theta)(T\cos\delta\theta - A) + (\cos\theta)(T\sin\alpha)]\frac{1}{m} + g_z$$
$$\ddot{\theta} = [-X_{cp}N_\alpha\sin(\alpha)) + X_{gim}T\sin\delta_\theta]/J_{yy}$$

where $\alpha = \theta + \gamma_\theta + \alpha_{w_\theta}$ is the effective angle of attack with $\gamma_\theta = \dot{z}/V$ the flight-path (drift) angle. Due to the study is centered on the attitude control of the rocket during the descent phase, in this paper, we use the equations of height (z) and attitude pitch (θ) only. That is:

$$\begin{aligned} \ddot{z} &= (T\cos(\delta\theta) - A)\frac{\sin(\theta)}{m} \quad (23) \\ &\quad +(T\sin\delta\theta - N_\alpha\sin(\alpha))\frac{\cos(\theta)}{m} \\ &\quad -\frac{\mu}{r^2}[1+\frac{3}{2}j_2(\frac{R_0}{r})^2(3-5(\frac{z}{r})^2)]\frac{z}{r} \\ \ddot{\theta} &= [-X_{cp}N_\alpha\sin(\alpha) + X_{gim}T\sin(\delta_\theta)]/J_{yy} \quad (24) \end{aligned}$$

Given that TVC is applied to small angles ($\approx 4° - 15°$), we assume $\sin(x) = x$ and $\cos(x) = 1$, we have that rewriting (23)-(24) in state-space, with $\alpha_{w_\theta} = 0$, the rocket dynamics will be defined as

$$\dot{x} = f(*)x + g(*)\delta\theta \quad (25)$$

where $\mathbf{x} = [x_1 = z, x_2 = \dot{z}, x_3 = \theta, x_4 = \dot{\theta}]^T \in \Re^4$, $\delta\theta$ is the rocket thrust vector control,

$$f(*) = \begin{bmatrix} 0 & 1 & 0 & 0 \\ g_z & \frac{N_\alpha}{mV} & \frac{T-A}{m} - \frac{N_\alpha}{m} & 0 \\ 0 & 0 & 0 & 1 \\ 0 & -\frac{X_{cp}N_\alpha}{V} & 0 & -\frac{X_{cp}N_\alpha}{J_{yy}} \end{bmatrix}$$

$g(*) = [0, \frac{T}{m}, \frac{X_{gim}T}{J_{yy}}]^T$ with $g_z = -\frac{\mu}{r^2}[1+(\frac{9}{2}j_2(\frac{R_0}{r}))^2]\frac{z}{r}$ for $-\frac{15}{2}j_2(\frac{R_0}{r})^2(\frac{z}{r})^2 \approx 0$. Now, we are in conditions to proceed to design a controller to regulate the angle of attack using (25).

3 CONTROLLER DESIGN

Notice that (25) is not in a lower triangular form such that approach as backstepping can not be applied. Assuming that some aircraft parameters are not entirely known and the wind speed is uncertain, this paper proposes a sliding-mode-based TVC.

To control the flight-path angle, γ_θ and the pitch angle θ simultaneously through the TVC, we propose a control law as

$$\delta\theta = 1/g_2(-K_d sign(S_1)) \tag{26}$$

where $S_1 = x_1 + x_4$ represents the sliding surface, $g_2 = \frac{X_{gim}T}{J_{yy}}$, and $K_d > 0$ as feedback gain. From SMC theory, to guarantee switching, the condition $S_1\dot{S}_1 < 0$ should be satisfied, [4].

Proposition: Consider (26) to control a flight-path, z angle and pitch angle θ in a rocket. Then convergence to the origin is assured, in finite time $t_f = \frac{|S_1(t_0)|}{\sigma}$, if K_d is large enough for any practical initial conditions.

Proof: Consider the following Lyapunov function $V = 1/2S_1^2$ whose total derivative is given as

$$\begin{aligned}
\dot{V} &= S_1\dot{S}_1 = S_1(\dot{x}_1 + \dot{x}_4) \\
&= S_1(x_2 - \frac{X_{cp}N_\alpha}{V}x_2 - \frac{X_{cp}N_\alpha}{J_{yy}}x_4 + \frac{X_{gim}T}{J_{yy}}\delta\theta) \\
&= S_1([1 - \frac{X_{cp}N_\alpha}{V}]x_2 - \frac{X_{cp}N_\alpha}{J_{yy}}x_4 + \frac{X_{gim}T}{J_{yy}}\delta\theta) \\
&= S_1([1 - \frac{X_{cp}N_\alpha}{V}]x_2 - \frac{X_{cp}N_\alpha}{J_{yy}}x_4 - K_d sign(S_1)) \\
&\leq -K_d|S_1| + |S_1|(\Lambda_1 + \Lambda_2) = -K_d|S_1| + |S_1|\Lambda \\
&\leq -\sigma|S_1| \quad \forall S_1 \neq 0
\end{aligned} \tag{27}$$

where $\sigma = K_d - \Lambda$,$|[1 - \frac{X_{cp}N_\alpha}{V}]||x_2| \leq \Lambda_1$, $\frac{X_{cp}N_{alpha}}{J_{yy}}||x_4 \leq \Lambda_2$, with $\Lambda_1 > 0$, $\Lambda_2 > 0$, $|x_2| \leq V_{x2}$ and $|x_4| \leq V_{x4}$. Hence, in order to prove that $S_1 \to 0$ in finite time, we can always choose $K_d > \Lambda$ in such a way that $\sigma > 0$ guarantees the existence of a sliding mode at $S_1 = 0$ at time $t_f = \frac{|S_1(t_0)|}{\sigma}$. Thus, a trivial solution that satisfy $S_1 = 0$ is given as $x_1 = x_4 = 0$, i.e. $z = \dot{\theta} = 0$.

4 NUMERICAL RESULTS

In this section, we present the numerical results to show the performance of the proposed controller (26) under different conditions. The simulations were conducted on Python under Windows 10©. The parameters of the rocket used in the simulations are $N_\alpha = 4.46477N$, $A = 6.09525N$, $m = 570 \times 10^3 kg$, $T = 7.605 \times 10^6 N$, $X_{gim} = 21m$, $X_{c.p.} = 10m$, $J_{yy} = 3.2 \times 10^7 kgm^2$, $J_2 = 1.0826 \times 10^{-3}$, $\mu = 3.986 \times 10^14 \frac{m^3}{s^2}$, $R_0 = 6.371 \times 10^6 m$, $r = 6.372 \times 10^6 m$ and $V = 400\frac{m}{s}$, [16]. The simulation's goal is to guarantee the control of the angle of attack by assuring the convergence of the flight path and the pitch angle. The initial conditions used in the simulations are: $z = \dot{z} = \dot{\theta} = 0$ with

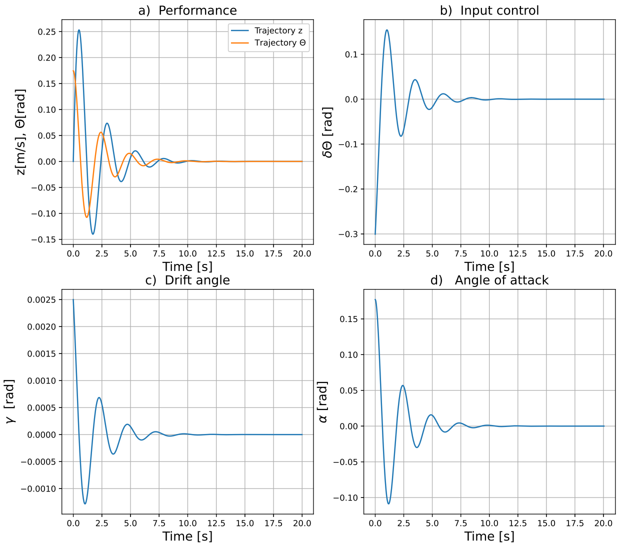

Figure 7: a) Performance under $\alpha_{w\theta} = 0$, b) TVC input control (δ_θ), c) Drift angle (γ), d) Angle of attack (α)

$\theta = 0.17453$. Finally, for simulations, was used a feedback gain of $K_d = 10$.

In the first simulation, we consider that the wind disturbance is zero, that is, $\alpha_{w_\theta} = 0$. In Figure 7 a) we observe how the states z, θ converge to the desired value 0, while in Figure 7 b) we show the performance of the TVC input control (δ_θ) within the band of the angle allowed. Figure 7 c) and d) are shown how the drift angle and angle of attack tend to zero, respectively. Notice the convergence relations between z, θ and γ, α, respectively. In the second simulation is proposed two kind of wind disturbances. In the first case the wind disturbance is defined as $\alpha_{w\theta} = \sin(\eta t) + \Delta$ with $\eta = 2$ and $\Delta = 3$, see Figure 8. As in previous case we can notice the robustness of the controller to compensate the parametric uncertainty and the disturbances. In the second case, see Figure 9, we assume that the wind disturbance is defined as a Gaussian noise, that is, $\alpha_{w\theta} = \frac{1}{(2\pi\epsilon^2)}e^{\frac{-(o-\zeta)^2}{(2\epsilon^2)}}$ where $\epsilon = 1$, $\zeta = 0.03$. As previously, we can notice that the controller can compensate the disturbance and guarantee the convergence of the θ and $\dot{z}$ to zero.

A comparative performance indices of the proposed controller and LQR controller is presented in Table 1 where ISE represents the Integral Square Error and IAE the Integral Absolute Error.

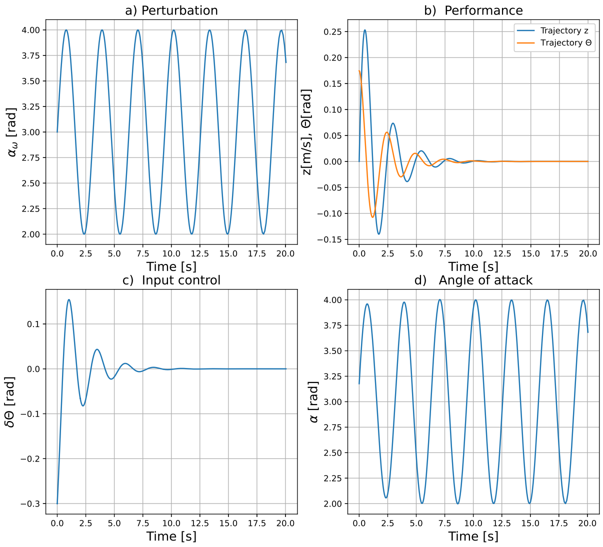

Figure 8: a) Wind disturbance α_{w_θ} as a sinusoidal function, b) Performance including wind disturbance, c) TVC input control, d) Angle of attack

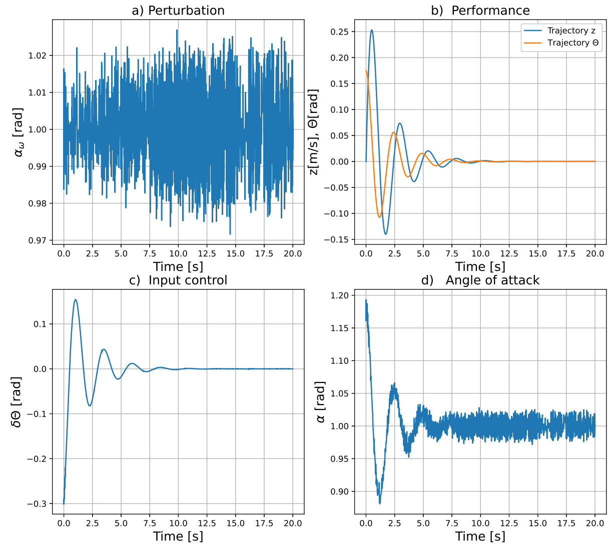

Figure 9: a) Wind disturbance $\alpha_{w\theta}$ as a gaussian function, b) Performance including wind disturbance, c) TVC input control, d) Angle of attack

Table 1. Performance Indices: ISE,IAE

Proposed	$ISE_\theta = 0.0147$	$ISE_z = 0.0756$
	$IAE_\theta = 0.1962$	$IAE_z = 0.4807$
LQR	$ISE_\theta = 0.0439$	$ISE_z = 0.0376$
	$IAE_\theta = 0.3669$	$IAE_z = 0.3242$$

5 Conclusion

A complete dynamical model of the rocket, using a TVC, is presented. A reduced dynamical of the rocket is proposed to control the angle of attack, which allows us to reduce the drift in flight through TVC. A model-free sliding-mode-based TVC is presented to guarantee robustness in the presence of parametric uncertainties and wind disturbances. As a part of the Master thesis in Aerospace Engineering at Universidad Politecnica Metropolitana de Hidalgo, Mexico, an experimental rocket is being developed to validate the proposed approaches, see Figure 10.

Acknowledgements

This work was partially supported by CONACYT Scholarships with reference number 0055803.

References

[1] T. Devlin, R. Dickerhoff, K. Durney, A. Forrest, P. Pansodtee, A. Adabi and M. Teodorescu, ElbowQuad: Thrust Vectoring Quadcopter, 2018 AIAA Information Systems-AIAA Infotech @ Aerospace 8–12 January 2018, Kissimmee, Florida. https://doi.org/10.2514/6.2018-0893

[2] J.P. Silva, C. De Wagter, and G. de Croon, Quadrotor Thrust Vectoring Control with Time and Jerk Optimal Trajectory Planning in Constant Wind Fields, Unmanned Systems, vol. 06(01), pp.15-37, 2018. doi.org/10.1142/S2301385018500024.

[3] X. Wang, B. Zhu, J. Zhu, et al. Thrust vectoring control of vertical/short takeoff and landing aircraft. Sci. China Inf. Sci. 63, 124202 (2020). doi.org/10.1007/s11432-018-9795-y.

[4] J. Y. Hung, W. Gao and J. C. Hung, Variable structure control: a survey, IEEE Transactions on Industrial Electronics, vol. 40(1), pp. 2-22, 1993. doi: 10.1109/41.184817.

[5] R. A. DeCarlo, S. H. Zak and G. P. Matthews, Variable structure control of nonlinear multivariable systems: a tutorial, Proceedings of the IEEE, vol. 76(3), pp. 212-232, 1988. doi: 10.1109/5.4400.

[6] M. Sharma, D.W. Ward, Flight-Path angle control via neuro-adaptive backstepping, AIAA Guidance, Navigation, and Control Conference and Exhibit, 05 August 2002 - 08 August 2002 Monterey, California, USA. doi.org/10.2514/6.2002-4451.

Figure 10: Experimental rocket plane, Universidad Politecnica Metropolitana de Hidalgo.

[7] S.-H. Yoon, Y.-D. Kim, and S.-H. Park, Constrained adaptive backstepping controller design for aircraft landing in wind disturbance and actuator stuck, International Journal of Aeronautical and Space Sciences. The Korean Society for Aeronautical & Space Sciences, 13(1), pp. 74–89. doi: 10.5139/ijass.2012.13.1.74.

[8] B. Choi, HJ. Kim, and Y. Kim, Robust control allocation with adaptive backstepping flight control. Proceedings of the Institution of Mechanical Engineers, Part G: Journal of Aerospace Engineering, vol. 228(7), pp. 1033-1046, 2014. doi:10.1177/0954410013483687.

[9] Ma. Ran, Q. Wang, D. Hou, C. Dong, Backstepping design of missile guidance and control based on adaptive fuzzy sliding mode control, Chinese Journal of Aeronautics, vol. 27(3), pp. 634-642, 2014. doi.org/10.1016/j.cja.2014.04.007.

[10] Li, Q., Zhang, W., Han, G. and Y. Yang, Adaptive neuro-fuzzy sliding mode control guidance law with impact angle constraint. IET Control Theory Appl., 9: pp. 2115-2123, 2015. doi.org/10.1049/iet-cta.2014.1206

[11] Yuhang Yun, Shengjing Tang, Jie Guo and Yunqiang Zhou, Adaptive sliding-mode guidance with terminal angle constraints based on explicit space engagement model, IEEE Chinese Guidance, Navigation and Control Conference (CGNCC), 2016, pp. 1144-1147, doi: 10.1109/CGNCC.2016.7828949.

[12] W. Bong, D. Wie and W.Mark, Analysis and Design of Launch Vehicle Flight Control Systems, AIAA Guidance, Navigation and Control Conference and Exhibit, 2008. doi:10.2514/6.2008-6291.

[13] Ashish Tewari, Atmospheric and Space Flight Dynamics, 2007 Birkhauser, Boston-Basel-Berlin. ISBN-10: 0-8176-4437-7, doi: 10.1007/978-0-8176-4438-3

[14] Robert F. Stengel, Flight Dynamics, Princeton University Press, 2004, ISBN: 9781680159066, https://doi.org/10.2307/j.ctt1287kgx

[15] Enrique C. del Rio, Cinemática Y Dinámica del Sólido Rigido, Padre Benito Menni-6-2-E 47008 Valladolid, España.

[16] Lusting Matias, Modeling of Launch Vehicle during the Lift-of Phase in Atmosphere, Bachelor's Thesis, Czech Technical University in Prague, May 18, 2017